Biomineralization Behavior of a Vinylphosphonic acid-based Copolymer Added with Polymerization Accelerator in Simulated Body Fluid

Ryo Hamai[1], Yuki Shirosaki[2] and Toshiki Miyazaki[1,*]

[1]Graduate School of Life Science and Systems Engineering, Kyushu Institute of Technology, Japan

[2]Frontier Research Academy for Young Researchers, Kyushu Institute of Technology, Japan

*** Corresponding author:**

Toshiki Miyazaki

Graduate School of Life Science and Systems Engineering, Kyushu Institute of Technology, 2-4, Hibikino, Wakamatsu-ku, Kitakyushu 808-0196, Japan

Tel/Fax: +81-93-695-6025

E-mail: tmiya@life.kyutech.ac.jp

Abstract

Apatite-polymer composites have been evaluated in terms of its potential application as bone substitutes. Biomimetic processes using simulated body fluid (SBF) are well-known methods for preparation of such composites. They are reliant on specific functional groups to induce the heterogeneous apatite nucleation and phosphate groups possess good apatite-forming ability in SBF. Improving the degree of polymerization is important for obtaining phosphate-containing polymers, because the release of significant quantities of monomer or low molecular weight polymers can lead to suppression of the apatite formation. To date, there have been very few studies pertaining to the effect of adding a polymerization accelerator to the polymerization reaction involved in the formation of these composite materials under physiological conditions. In this study, we have prepared a copolymer from triethylene glycol dimethacrylate and vinylphosphonic acid (VPA) in the presence of different amounts of sodium *p*-toluenesulfinate (*p*-TSS) as a polymerization accelerator. The effects of *p*-TSS on the chemical durability and apatite formation of the copolymers were investigated in SBF. The addition of 0.1–1.0 wt% of *p*-TSS was effective for suppressing the dissolution of the copolymers in SBF, whereas larger amount had a detrimental effect. A calcium polyvinylphosphate instead of the apatite was precipitated

in SBF.

Highlights

(1) Effects of polymerization accelerator of P-containing copolymers have been clarified.

(2) Chemical durability has been significantly improved by the accelerator addition.

(3) All the phosphate groups do not induce the apatite formation in SBF.

Keywords

Simulated body fluid, Biomimetic process, Organic-inorganic composites, Phosphate group, Sodium *p*-toluenesulfinate

1. Introduction

Bioglass [1], glass-ceramics A-W [2] and sintered hydroxyapatite [3] have been used as bone substitutes because all three of these ceramic materials can bond directly to living bone. This unique property of these materials is referred to as bioactivity and these ceramics are therefore known as bioactive ceramics. However, bioactive ceramics generally have a higher Young's modulus than living bone, which can cause mechanical stress at the bone interface and increase the likelihood of the surrounding living bone being absorbed because of stress-shielding after the implantation. Living bone is an organic-inorganic composite consisting of apatite and collagen fiber, and it is therefore expected that novel bone substitute composites should not only exhibit bioactivity properties similar to those of living bone, but also show similar mechanical properties.

Biomimetic processes involving simulated body fluid (SBF) have been developed as effective methods for the preparation of organic-inorganic composites [4]. According to these processes, specific functional groups are positioned on the surface of an organic material where they play an important role in inducing the heterogeneous nucleation of apatite to give an organic-inorganic composite. A variety of different functional groups, including Si-OH [5], Ti-OH [6], Ta-OH [7], -COOH [8], -SO_3H [9], and -PO_3H_2 (phosphate) [8], have been reported to induce the nucleation of apatite in SBF.

Tanahashi *et al*. investigated the effect of several different functional groups in terms of their ability to induce the growth apatite crystals on self-assembled monolayers in SBF. The results of this particular study showed that phosphate groups had good apatite-forming ability [8]. Based on this result, it is envisaged that the introduction of phosphate groups to an organic polymer would provide an effective strategy for the preparation of apatite-polymer composites via a biomimetic process. Furthermore, it is envisaged that the formation of apatite on polymers with a high cross-linking density will provide access to high-strength composites.

Phosphate-containing vinyl monomers such as vinylphosphonic acid (VPA) have been used extensively as precursors for the formation of apatite-polymer composites in a wide range of biomaterial applications. For example, Tan *et al*. reported the preparation of a VPA-acrylamide copolymer that enhanced the adhesion and growth rate of osteoblast-like cells [9,10]. Stancu *et al.* reported the preparation copolymers from methacryloyloxyethyl phosphate and (diethylamino)ethyl methacrylate [11]. The same authors went on to report the formation of calcium phosphate in SBF, although these results were not confirmed spectroscopically with the apatite.

Phosphate-containing monomers can inhibit radical polymerization processes initiated by the combination of peroxide or camphor quinone with a tertiary amine,

because the monomers can form a salt with the tertiary amine [12, 13]. Furthermore, the dissolution of monomers or low molecular weight polymers can disfavor the formation of apatite by causing a decrease in the pH of the surrounding fluid. It has been reported that sodium *p*-toluenesulfinate (*p*-TSS) can be used to promote the radical polymerization of phosphate-containing monomers for the preparation of dental resins [14]. Na^+ ions in *p*-TSS are exchanged with H^+ ions of acidic monomer [15]. This reaction inhibits the formation of the salt and more amount of tertiary amine can contribute the radical production. Thus polymerization of phosphate containing monomer is promoted.

However, the effect of the addition of an accelerator on the biomineralization behavior of a copolymer in simulated body fluid remains unclear. Furthermore, several other factors can affect the dissolution and degradation of copolymers of this type, including the molecular weight, crosslink density and hydrophilicity of the copolymer [16, 17].

In the current study, effects of the *p*-TSS addition on calcification behavior on the surface of VPA-based copolymer were investigated in SBF in terms of its chemical structure and surface reaction.

2. Materials and methods

2.1 Preparation of the polymers samples

All of the reagents were used in the current study were purchased from commercial suppliers and used without further purification. VPA (95%, Tokyo Chemical Industry Co., Ltd, Tokyo, Japan) and triethylene glycol dimethacrylate (TEGDMA, 90%, Wako pure Chemical Industries, Ltd, Osaka, Japan) were used as the monomers at a VPA:TEGDMA weight ratio of 1:3.98. Different amounts of *p*-TSS (98%, Tokyo Chemical Industry Co., Ltd) were dispersed in the mixture of VPA and TEGDMA monomers described above at 0–5.0 wt% to the total amount of VPA and TEGDMA using an ultrasonic cleaner. The photo polymerization initiator *N*,*N*'-dimethyl-*p*-toluidine (97%, Wako Pure Chemical Industries, Ltd) and (±)-camphorquinone (97%, Wako Pure Chemical Industries, Ltd) were then added at concentrations of 2 and 0.77 wt%, respectively, relative to the total amount of monomers in the mixture.

The mixtures were then stirred in the absence of light for 1 h, and then exposed to blue light (460 nm) for 1 h to progress the polymerization reactions. The resulting copolymer products were then dried at 60°C for 1 day before being soaked in ultra-pure water for 1 day at room temperature to remove any unreacted monomers. After being

dried for 24 h at 60°C, the copolymer products were cut into square pieces of 10 x 10 x 1 mm in size and polished using waterproof abrasive paper (SiC #1000).

2.2 Preparation of SBF and soaking specimen in SBF

SBF (Na^+ 142.0, K^+ 5.0, Mg^{2+} 1.5, Ca^{2+} 2.5, Cl^- 147.8, HCO_3^- 4.2, HPO_4^{2-} 1.0, SO_4^{2-} 0.5 mM (M = kmol・m^{-3})) was prepared by adding NaCl, $NaHCO_3$, KCl, $K_2HPO_4 \cdot 3H_2O$, $MgCl_2 \cdot 6H_2O$, $CaCl_2$, and Na_2SO_4 (Nacalai Tesque, Inc., Kyoto, Japan) to one pot of ultra-pure water in this order. The pH of the resulting solution was adjusted to 7.40 by the addition of tris(hydroxymethyl) aminomethane (Nacalai Tesque, Inc.) and the appropriate volume of a 1 M hydrogen chloride solution. The polymers samples prepared above were then soaked in 30 mL of SBF at 36.5°C for various time periods over a maximum of 7 days.

2.3 Characterization

The polymer samples were analyzed by scanning electron microscopy using a scanning electron microscope (SEM, S-3500N, Hitachi Co., Tokyo, Japan) equipped with an energy dispersive X-ray (EDX) analysis system (EMAX Energy, Horiba Ltd, Kyoto, Japan). The samples were also analyzed by powder and thin-film X-ray

diffraction (TF-XRD; MXP3V, Mac Science, Co., Yokohama, Japan) and Fourier transform infrared spectroscopy (FT-IR; FT/IR-6100, JASCO Co., Tokyo, Japan) using an attenuated total reflectance method. For the TF-XRD analysis, the angle of the X-ray (CuKα) was fixed at 1° relative to the surface of the sample. For the SEM-EDX analysis, the surfaces of the samples were coated with carbon using a carbon coater (CADE, Meiwafosis Co., Ltd., Osaka, Japan). The hydrophilicities of the surfaces of the different samples were evaluated using a water-contact angle gauge (DMe-200, Kyowa Interface Science, Co., Ltd., Saitama, Japan). The glass-transition temperature (T_g) of each sample was measured by differential scanning calorimetry (DSC; DSC 3100S, Mac Science, Co., Yokohama, Japan). During the DSC measurement, the samples were heated from room temperature to 200°C at a rate of 10°C/min. Moreover, the initiation temperature of thermal decomposition of samples was evaluated by thermal thermogravimetric analysis (TG; TG-DTA 2000S, Mac Science, Co., Yokohama, Japan). During the TG analysis, the sample was heated at a rate of 10°C/min.

The concentrations of Ca and P in the SBF following the soaking of the different polymer samples were determined by inductively coupled plasma optical emission spectrometry (ICP-OES; Optima 4300DV CYCLON, Perkin-Elmer Inc., London, UK). The pH of the SBF was also measured following the soaking procedure using a pH

meter (F-23IIC, Horiba Ltd.).

3. Results

Figure 1 shows the results for the phosphorus content and the water contact angles for the surfaces of the different copolymer samples treated with different amounts of *p*-TSS. The results revealed that the P content of the copolymer samples increased and the contact angle decreased as the amount of *p*-TSS increased. Figure 2 shows the DSC curves of the different copolymer samples and the corresponding T_g values. The baseline of the curve slightly shifted to the side of endotherm due to the glass transition and the exothermic peak of crystallization appeared for all the samples. The results showed that the T_g values tended to increase as the amount of *p*-TSS increased. The initiation temperature of the thermal decomposition of the sample added with 0.1 and 5.0 wt% of *p*-TSS was 263.3 and 269.7^{o}C, respectively. This means that thermal stability of the copolymer is enhanced by *p*-TSS addition.

Figure 3 shows the SEM images of the different copolymer samples after they had been soaked in SBF for 7 days. The results revealed that deposits had formed on the surfaces of the copolymers containing 0.5 wt% or more *p*-TSS. Furthermore, the size of these deposits increased as the amount of *p*-TSS added to the polymerization increased.

From a magnified SEM image of the deposits formed with 5.0 wt% *p*-TSS, it was clear that the deposits were composed of fine spherical particles with diameters in the range of 300 nm to 1 μm. Subsequent EDX analysis revealed that the depositions contained Ca and P, and that the molar ratio of Ca/P was about 3:2 for all the of copolymer samples tested.

Figure 4 shows the TF-XRD patterns of the different copolymer samples after they had been soaked in SBF for 7 days. The results revealed that no diffraction peaks were observed for any of the copolymer samples prepared in the current study. In the powder XRD pattern of samples containing 5.0 wt% of *p*-TSS before and after soaked in SBF for 7 days, the broad halo patterns characteristic to the amorphous phase were only observed in both patterns (data not shown).

Figure 5 (A) shows the FT-IR spectra of the different copolymer samples prepared in the current study prior to being soaked in SBF. Two peaks were observed at 930 and 990 cm^{-1} in all of the samples, which were attributed to the P–O bonds. An additional peak was observed at 1150 cm^{-1} for all of the copolymer samples before soaking in SBF, which was assigned to the P=O groups. Peaks corresponding to C-O-C stretching vibrations were also observed at 1030, 1130 and 1160 cm^{-1}, as well as a peak at 1720 cm^{-1}, which was attributed to a C=O stretching vibration.

After they had been soaked in SBF for 7 days as shown in Fig. 5(B), the intensity of the band corresponding to the C=O peaks derived from the TEGDMA monomer decreased over time, whilst a new peak corresponding to the P–O bond in the $–PO_3^{2–}\cdots Ca^{2+}$ complex appeared at 889 cm^{-1} for the specimens added with 3.0 and 5.0 wt% *p*-TSS [18].

Figure 6 shows the changes in the P, Ca concentrations and pH of the SBF following the soaking of the different copolymer samples for various periods of time. Minor increases in the P concentration were observed when the specimen contained 0.1, 0.5 and 1.0 wt% *p*-TSS. In contrast, significant increases in the P concentration were observed for the copolymer samples treated with 3.0 and 5.0 wt% *p*-TSS. The Ca concentration of the SBF decreased monotonically for all of the copolymer samples prepared in the current study after they had been soaked. Copolymer samples containing high *p*-TSS contents showed a greater tendency towards the adsorption of large amounts of Ca^{2+} in SBF. The pH values of the SBF following the soaking of the copolymer samples containing 0.1, 0.5 and 1.0 wt% *p*-TSS were higher than that of the sample containing 0 wt% *p*-TSS. In contrast, the pH values of the SBF following the soaking of the copolymers containing 3.0 and 5.0 wt% *p*-TSS were lower than that of the sample containing no *p*-TSS.

4. Discussion

The copolymerization reactions of VPA and TEGDMA reached completion reached completion regardless of the amount of *p*-TSS added to the reaction, as evidenced by the lack of peaks corresponding to the C=C bonds of the uncured VPA and TEGDMA monomers (see Figure 5 (A)). Despite the fact that the initial VPA content remained constant regardless of the amount of *p*-TSS added to the reaction, the amount of phosphorus incorporated into the different copolymers was different, as shown in Figure 1. The increase in phosphorus content indicates the accelerated polymerization of VPA. It is assumed that *p*-TSS react with VPA as shown in equation 1, inhibit the formation of NDT-VPA salt and finally promote the radical polymerization.

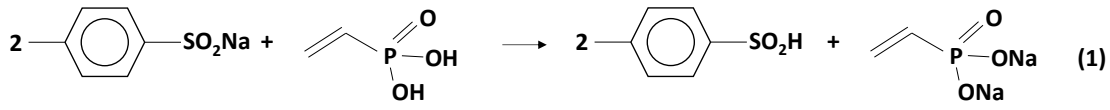

(1)

This result indicated that it was becoming increasingly difficult to wash any phosphorus-containing compounds from the polymerized VPA after it had been treated with *p*-TSS and soaked in ultrapure water. The dissolution of phosphorus-containing molecules from the copolymer and the decrease in the pH of the SBF were suppressed

significantly by the addition of 0.1–1.0 wt% of *p*-TSS, although the addition of even larger amounts of *p*-TSS did not lead to further changes in these properties (see Figure 6). The solubility of a polymer generally decreases as it molecular weight and/or crosslink density increases. A high molecular weight or high crosslink density can also lead to an increase in the T_g value of a polymer [19]. The results of the current study showed that the T_g values of the copolymer products increased as the amount of *p*-TSS increased (see Figure 2), and it was therefore assumed that even the copolymers treated with 3.0 and 5.0 wt% *p*-TSS would have high crosslink densities. This is supported by TG results showing enhancement of thermal stability by *p*-TSS addition.

In this case, the hydrophilicity of the polymer would be expected to have a significant impact of the dissolution of the copolymer in SBF in a similar manner to the molecular weight and/or crosslink density. Yui *et al*. reported the preparation of a dental resin from bisphenol A diglycidyl ether dimethacrylate and 2-hydroxylethyl methacrylate. Notably, this highly hydrophilic resin was found to dissolve readily in pure water because of the enhanced diffusion of the water molecules to the resin and the subsequent cleavage of the hydrogen bonding interactions between the polymer chains [20]. Moreover, decreasing the pH of the resin led to the acid-catalyzed hydrolysis of the ester bond [21, 22]. The results of the current study revealed that the hydrophilicity

of the copolymer could be enhanced by increasing the *p*-TSS content, because this led to an increase in the phosphorus content on the surface of the copolymer (see Figures 1). The dissolution of the copolymer could therefore be enhanced by the acid-catalyzed cleavage of the ester bond of TEGDMA using a proton dissociated from the phosphate.

Deposits composed of Ca and P formed on the copolymers treated with 1.0–5.0 wt% *p*-TSS after they had been soaked in SBF for 7 days (see Figure 3). However, the morphology of these deposits was found to be different from that of the apatite formed on an organic polymer under simulated physiological conditions [9]. Although the formation of a $PO_3^{2-}\cdots Ca^{2+}$ complex was confirmed by FT-IR (See Figure 5 (B)), the P–O bond of an orthophosphate ion (PO_4^{3-}), which is characteristic of apatite and amorphous calcium phosphate was not observed [23]. In addition, no crystalline peaks were observed in powder XRD patterns. This suggests that the formed calcium polyvinylphosphate may be amorphous.

The results of this study therefore revealed that the calcium polyvinylphosphate was formed on the copolymer. The phosphate groups in the present specimens hardly contribute to the apatite formation in SBF, in spite that the decrease in pH of the SBF was suppressed. Tanahashi *et. al* reported that ion-ion interaction between phosphate group and Ca^{2+} induce excellent apatite nucleation on the surface of material [8].

Chemical structure of VPA is slightly different from the structure reported in the previous research. Namely, VPA is phosphonic acid-type (-C-P(O)$(OH)_2$), whereas the structure of the previously reported self-assembled monolayers is acid phosphate-type (-O-P(O)$(OH)_2$). Acidity of the phosphate is different by its chemical structure. Namely, the acidity of the former is lower than that of the latter [24]. Tanahashi *et al.* also claims that ion-ion interaction between functional group and Ca^{2+} gives higher apatite-forming ability than ion-polar or ion-nonpolar interaction in SBF. With this point in mind, it is assumed that VPA with lower acidity may hardly contribute to the heterogeneous nucleation of apatite in the SBF. Such structural effects should be investigated in more detail in future study.

5. Conclusions

The effects of *p*-TSS on the chemical durability and calcification of copolymer containing phosphate groups, which was prepared from VPA and TEGDMA, have been investigated in SBF. The addition of *p*-TSS at 1.0 wt% or less suppressed the dissolution of the VPA-TEGDMA copolymer in SBF, whereas the addition of larger amount of *p*-TSS had little to no effect. The copolymers precipitated calcium polyvinylphosphate in SBF, meaning that all the phosphate groups do not induce the

apatite nucleation. Further material design is therefore required to allow the stronger interaction Ca^{2+} and phosphate groups on the surface of the copolymer, because this may be important for inducing the apatite formation.

References

[1] L L. Hench, J. Am. Ceram. Soc., 81, 1705-–1728 (1998).

[2] T. Kokubo, H.M. Kim, M. Kawashita, Biomaterials, 24, 2161–2175 (2003).

[3] M. Jarcho, C.H. Bolen, M.B. Thomas, J. Bobick, J.F. Kay, R.H. Doremus, Hydroxyapatite synthesis and characterization in dense polycrystalline forms. J. Mater. Sci., 11, 2027–2035 (1976).

[4] C. Ohtsuki, M. Kamitakahara, T. Miyazaki, J. Tissue Eng. Regen. Med., 1, 33–38 (2007).

[5] S.B Cho, K. Nakanishi, T. Kokubo, N. Soga, T. Kamamura, T. Kitsugi, T. Yamamuro, J. Am. Ceram. Soc., 78, 1769–1774 (1995).

[6] M. Uchida, H.M. Kim, T. Fujibayashi, T. Nakamura, J. Biomed. Mater. Res. A, 64A, 164–170 (2003).

[7] T. Miyazaki, H.M. Kim, T. Kokubo, H. Kato, T. Nakamura, J. Sol-Gel Sci. Tech., 21, 83–88 (2001).

[8] M. Tanahashi, T. Matsuda, J. Biomed. Mater. Res., 34, 305–315 (1997).

[9] T. Kawai, C. Ohtsuki, M. Kamitakahara, T. Miyazaki, M. Tanihara, Y. Sakaguchi, S. Konagaya, Biomaterials, 25, 4529–4534 (2004).

[10] J. Tan, R.A. Gemeinhart, M. Ma, W.M. Saltzman, Biomaterials, 26, 2663–3671 (2005).

[11] I.C. Stancu, R. Filmon, C. Cincu, B. Marculescu, C. Zaharia, Y. Tourmen, M.F. Basle, D. Chappard, Biomaterials, 25, 205–213 (2004).

[12] F.R Tay, N.M King, B.I. Suh, D.H. Pashley, Arch. Orofac. Sci., 1, 36–41 (2006).

[13] R.L Bowen, E.N, Cobb J.E Rapson, J. Dent. Res., 61, 1070–1076 (1982).

[14] J. Yamauchi, J. Jpn. Soc. Dent. Mater. Devices, 5, 144–154 (1986) (in Japanese).

[15] K. Ikemura, T. Endo, J. Appl. Poly. Sci., 72, 1655-1668 (1999).

[16] A. Göpferich, Biomaterials, 17, 103–114 (1996).

[17] J. Malacarne, R.M. Carvalho, M.F. de Goes, N. Svizero, D.H. Pashley, F.R. Tay, C.K. Yiu, M.R.O. Carrilho, Dent. Mater., 22, 973–980 (2006).

[18] S. Jin, E. Gonsalves, J. Mater. Sci.: Mater. Med., 10, 363–368 (1999).

[19] S.L. Gibson, F.A. Landis, P.L. Drzal, Biomaterials, 27, 1711–1717 (2006).

[20] C.K.Y. Yui, N.M. King, M.R.O. Carrilho, S. Sauro, F.A. Rueggeberg, C. Prati, R.M. Carvalho, D.H. Pashley, F.R. Tay, Biomaterials, 27, 1695–1707, (2006).

[21] T.N.A.T. Rahima, D. Mohamada, H. M. Akilb, I.A. Rahmana, Dent. Mater., 28, 63–70 (2012).

[22] Y. Nishitani, K. Takahashi, Y. Hayashi, T. Hoshika, G. Horikawa, T. Nakata, K. Tanaka, H. Sano, M. Yoshiyama, Adhes. Dent., 26, 92–98 (2008) (in Japanese).

[23] P. Layrolle, A, Ito, T. Tateish, J. Am. Ceram. Soc., 81, 1421–1428 (1998).

[24] N. Moszner, U. Salz, J. Zimmermann, Dent. Mater., 21, 895-910 (2005).

Figure captions

Figure 1 Changes in phosphorus content and water contact angle on the surfaces of the samples added with *p*-TSS (N=3).

Figure 2 DSC curves and glass-transition temperatures (T_g) of the different copolymer samples treated with *p*-TSS .

Figure 3 SEM images of the surfaces of the different copolymer samples after they had been soaked in SBF for 7 days.

Figure 4 TF-XRD patterns of the surfaces of the different copolymer samples treated with *p*-TSS after they had been soaked in SBF for 7 days.

Figure 5 FT-IR spectra of the specimens added with *p*-TSS before (A) and after soaking in SBF for 7 days (B).

Figure 6 Changes in P, Ca concentrations and pH of SBF with soaking of the specimens (N=3).

Figure

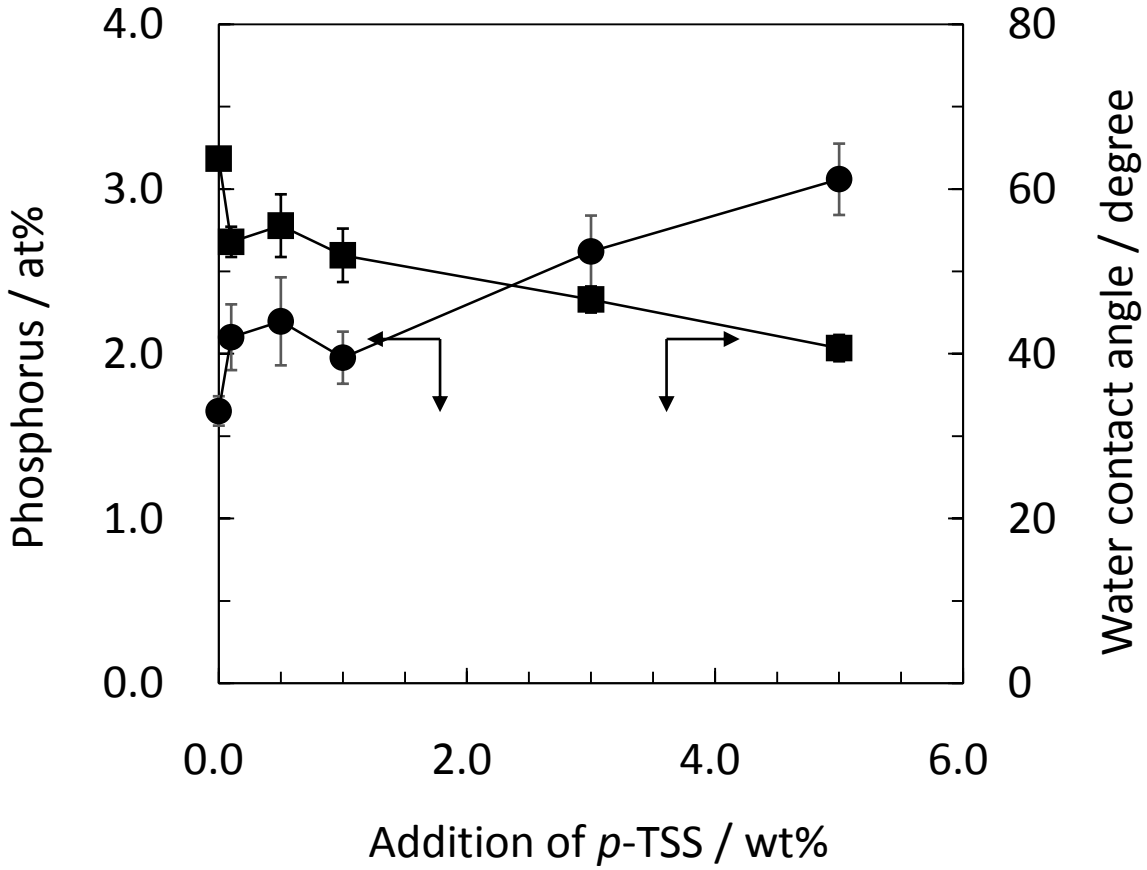

Figure 1 Changes in phosphorus content and water contact angle on the surfaces of the samples added with *p*-TSS (N=3).

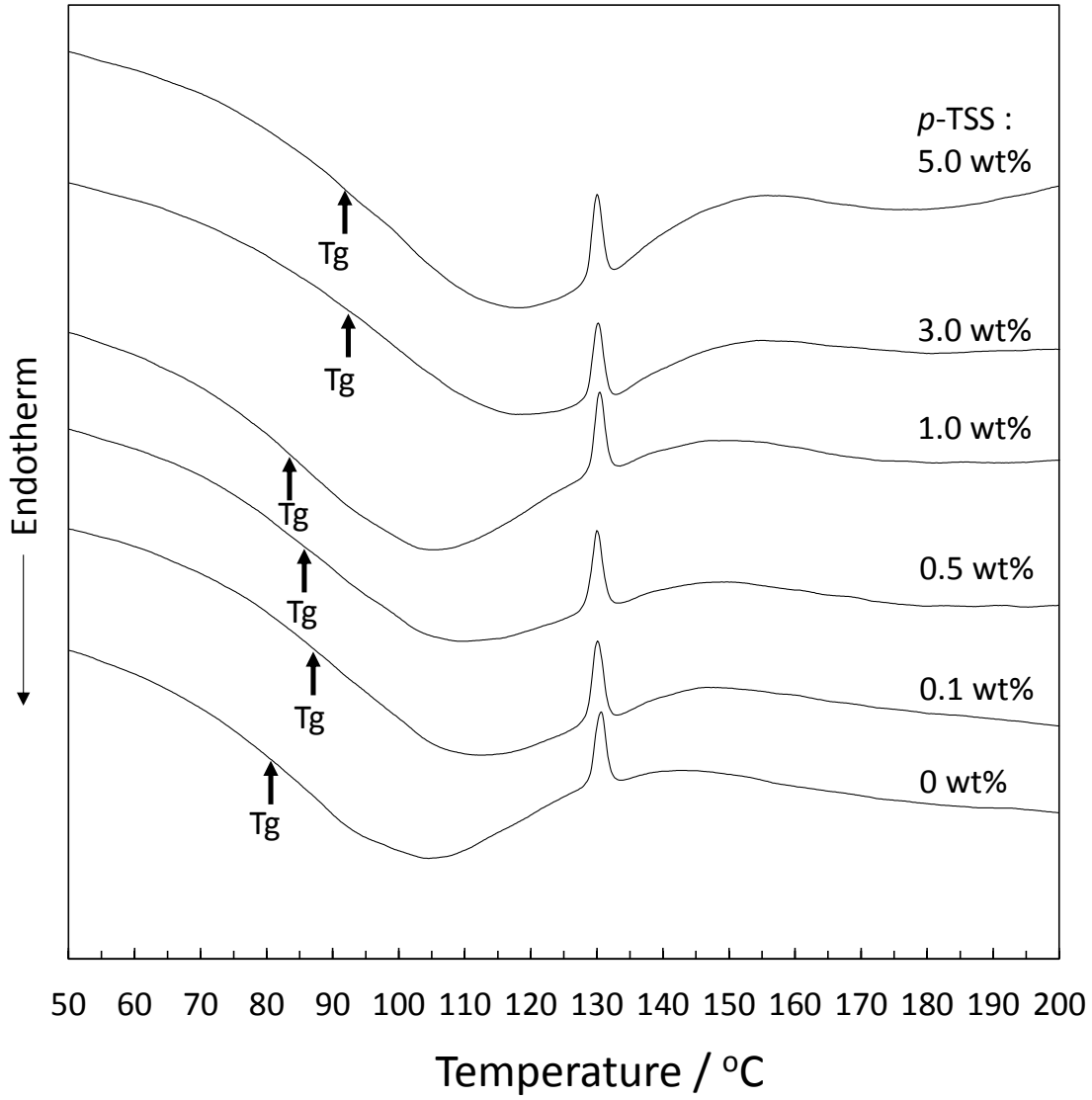

Figure 2 DSC curves and glass-transition temperatures (T_g) of the different copolymer samples treated with *p*-TSS .

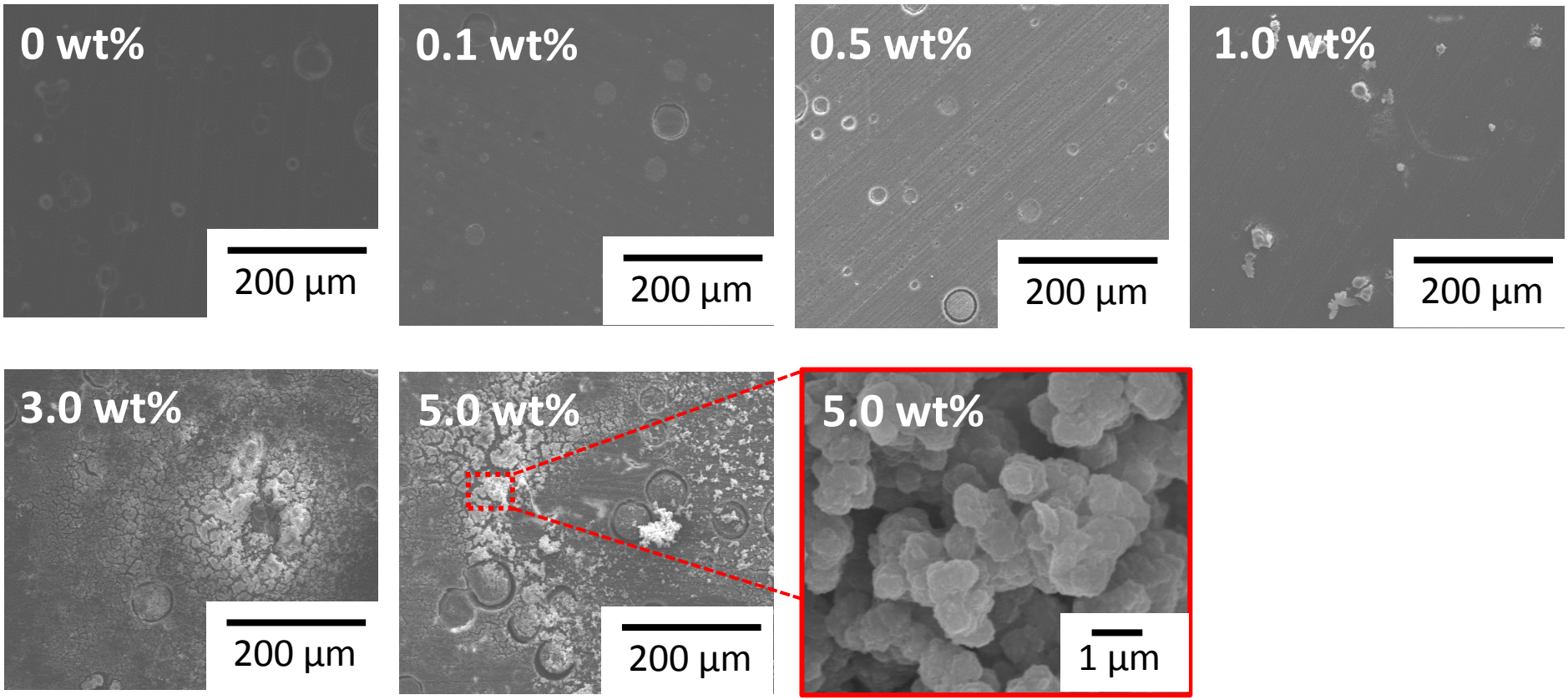

Figure 3 SEM images of the surfaces of the different copolymer samples after they had been soaked in SBF for 7 days.

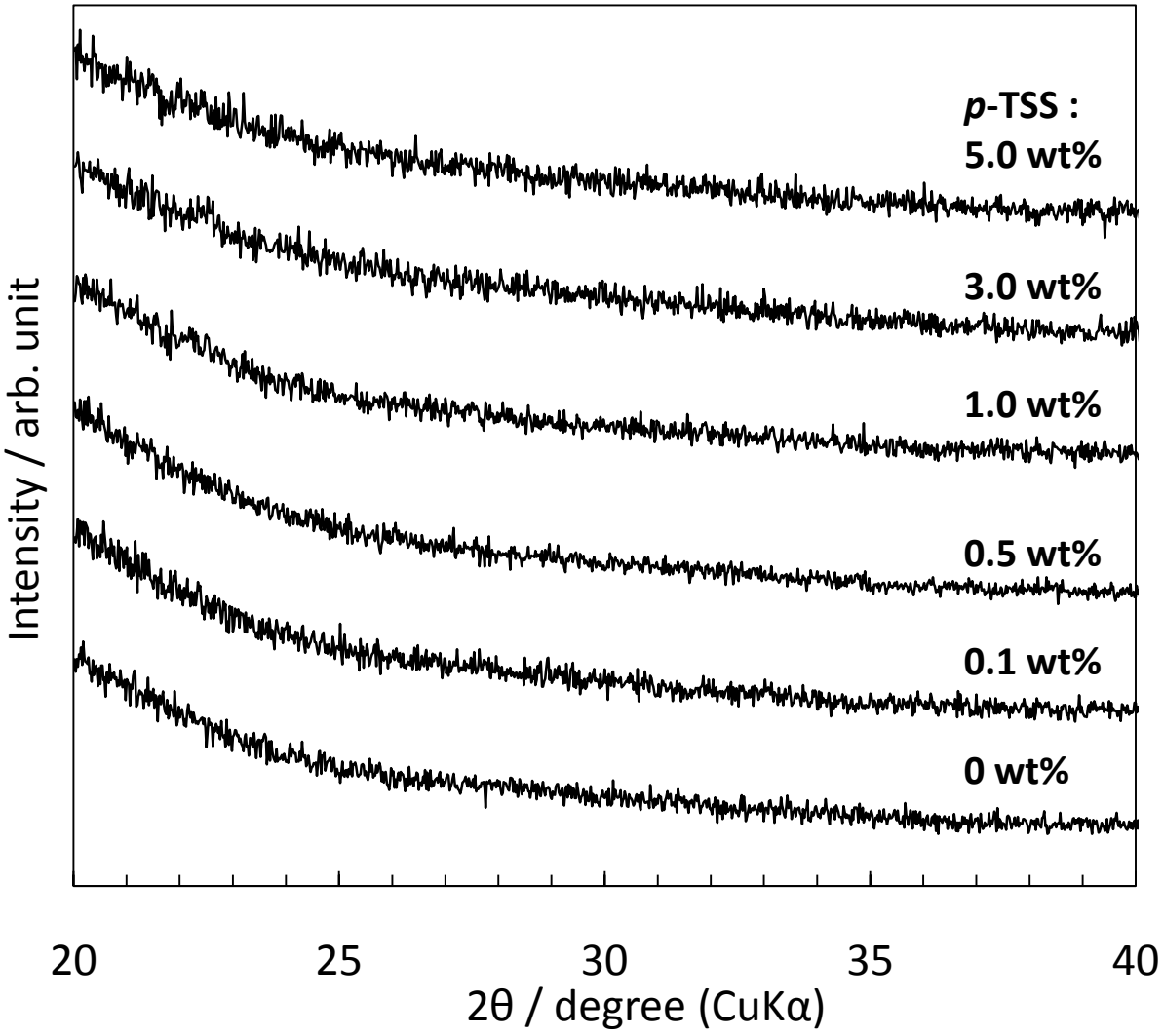

Figure 4 TF-XRD patterns of the surfaces of the different copolymer samples treated with *p*-TSS after they had been soaked in SBF for 7 days.

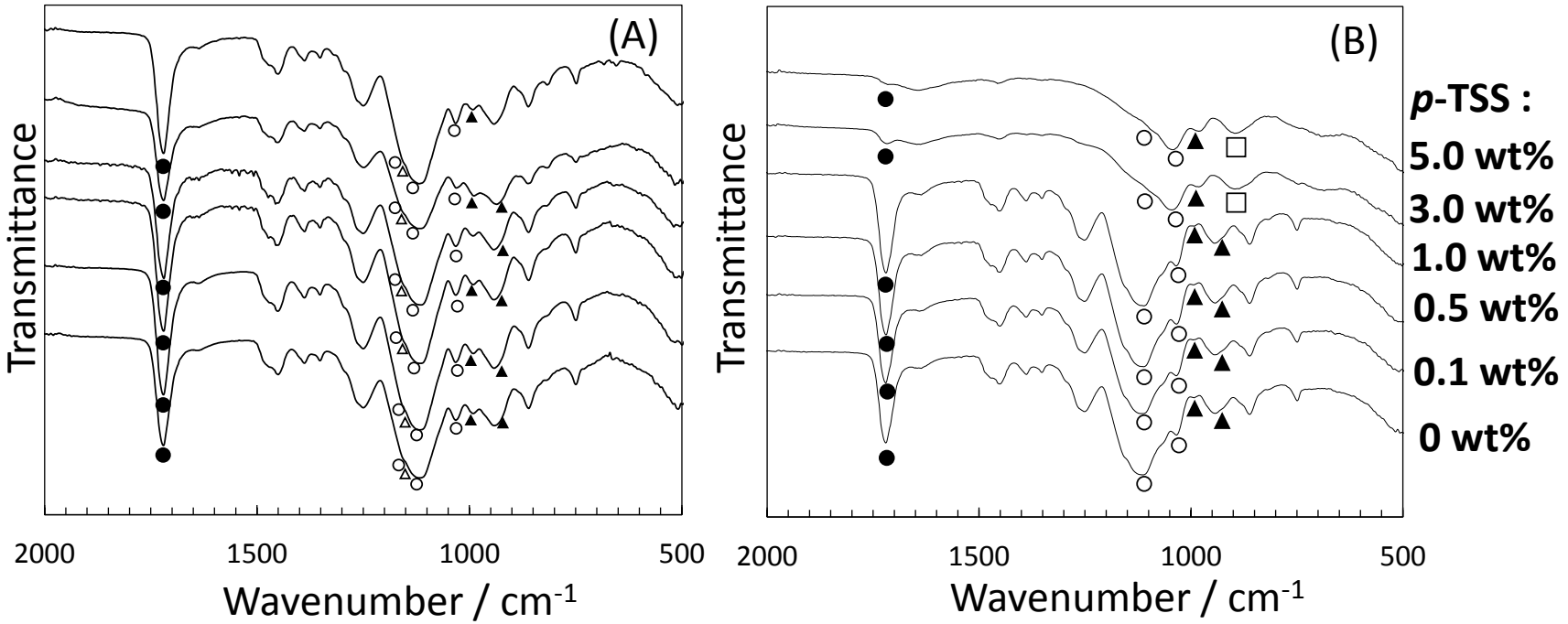

Figure 5 FT-IR spectra of the specimens added with *p*-TSS before (A) and after soaking in SBF for 7 days (B) (▲: P-O bond of VPA, △: P=O bond of VPA, ○: C-O-C bond of TEGDMA, ●: C=O bond of TEGDMA, □ : salt of $-PO_3^{2-}$ Ca^{2+}).

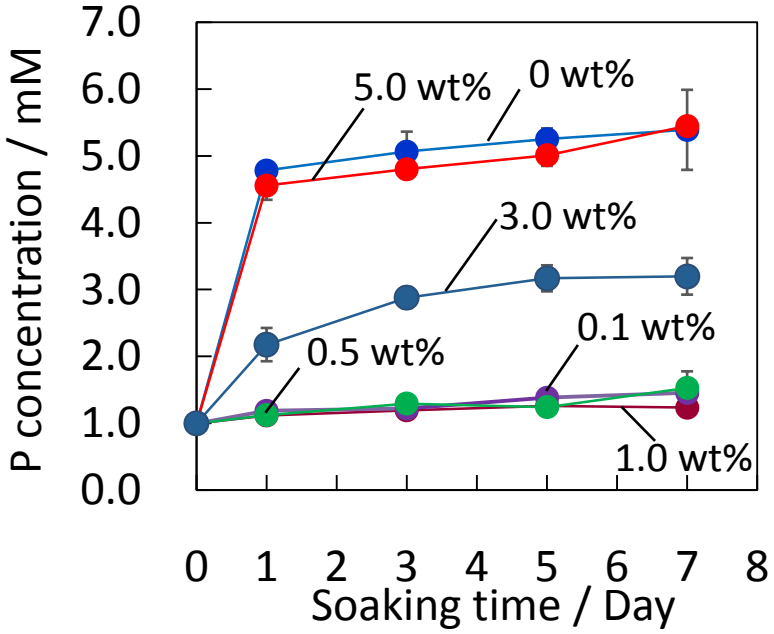

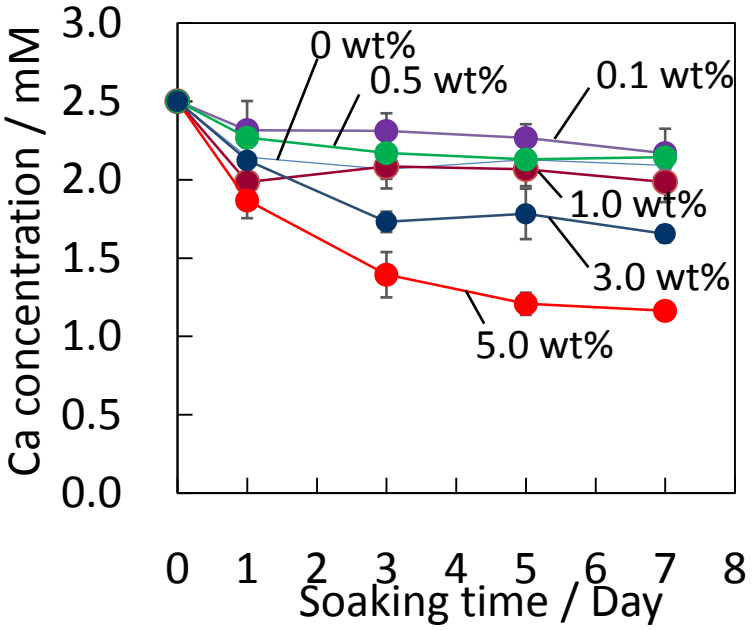

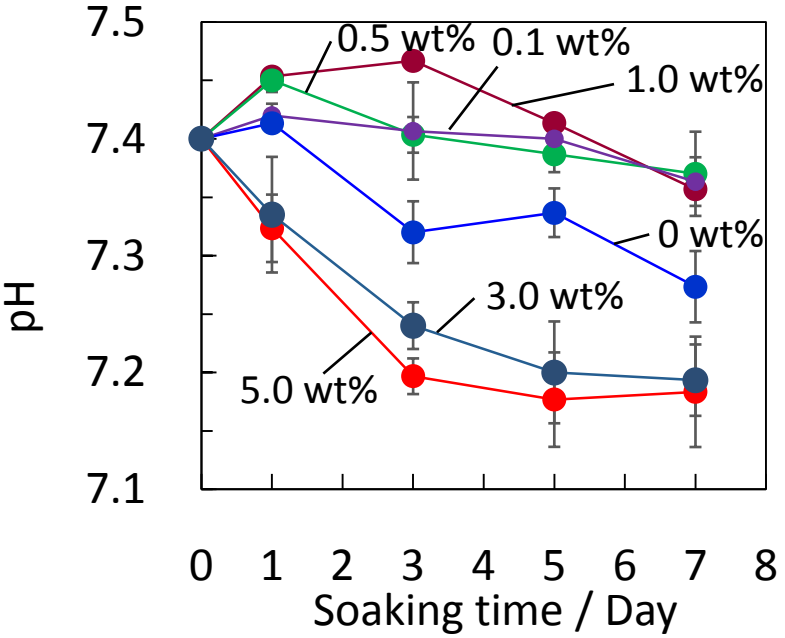

Figure 6 Changes in P, Ca concentrations and pH of SBF with soaking of the specimens (N=3).